GMR
The Original

Marine Bacterial Melanin-Conjugated Lipid Magnetic Nanoparticles And Its In-Vivo Anticancer Activity

Shilpa Valiyaparambil[1*], Janakiraman Kunchithapatham[1] Vinod K.R[2], Venkatesan P[1], Suresh B[1].

[1]Department of Pharmacy, Annamalai University, Annamalai Nagar, Chidambaram-608002, Tamil Nadu, India. janakiraman_k06@rediffmail.com, venkatesan1978@gmail.com, sure22chem@gmail.com
[2]Department of Pharmaceutics, Sanjo College of Pharmaceutics Studies, Vellapar, Palakkad, Kerala, India. vinodkr@gmail.com
*Corresponding author:Mrs Shilpa Valiyaparambil
Department of Pharmacy,Annamalai University, Annamalai Nagar,Chidambaram-608002,Tamil Nadu, India.
Email: shilpavp24@gmail.com

ABSTRACT
M-C-L-M-NPs were synthesized by chemical co-precipitation followed by lipid encapsulation and characterized using UV–Visible spectroscopy and HR-TEM. Male Wistar rats (n = 6/group) were divided into four groups: normal control, cancer control, 5-fluorouracil (20 mg/kg), and M-C-L-M-NPs (5 mg/kg). Skin carcinogenesis was induced using DMBA and croton oil for 16 weeks. Body weight, hematological parameters, inflammatory marker (TNF-α), and histopathological alterations were evaluated. Results: UV–Visible spectroscopy showed characteristic absorption between 250 and 380 nm, while HR-TEM confirmed spherical, uniformly distributed nanoparticles with minimal aggregation. Initial body weights were comparable among groups (147–153 g). At the end of the experiment, the cancer control group exhibited a marked reduction in body weight (≈123 g) compared with the normal control (≈179 g), whereas treatment with 5-fluorouracil (≈175 g) and M-C-L-M-NPs (≈177 g) preserved body weight. The M-C-L-M-NPs group showed the highest RBC count (≈5.8 × 10^6 cells/μL) and hemoglobin level (≈14.5 g/dL) compared with the cancer control (≈5.1 × 10^6 cells/μL; 10.8 g/dL). Serum TNF-α levels were markedly reduced from ≈43 pg/mL in the cancer control to ≈18 pg/mL following M-C-L-M-NPs treatment. Histopathological examination demonstrated substantial restoration of normal skin architecture with minimal inflammatory infiltration in the nanoparticle-treated group. Conclusion: Marine bacterial melanin-conjugated lipid magnetic nanoparticles exhibited superior anticancer efficacy, preserved hematological parameters, reduced inflammatory responses, and improved tissue architecture compared with conventional 5-fluorouracil, highlighting their potential as a promising nanotherapeutic platform for skin cancer treatment.

Keywords: Marine bacterial melanin, Lipid magnetic nanoparticles, Skin carcinogenesis, Anticancer activity, Nanomedicine.

INTRODUCTION

Cancer is one of the most serious global health problems and remains a leading cause of death despite continuous progress in medical science. It is characterized by the uncontrolled growth and spread of abnormal cells that invade surrounding tissues and eventually metastasize to distant organs. Although surgery, chemotherapy, radiotherapy, and immunotherapy have significantly improved cancer management, these treatments often suffer from several limitations, including poor target specificity, severe side effects, multidrug resistance, and toxicity to healthy tissues [1]. Conventional chemotherapeutic agents damage both malignant and rapidly dividing normal cells, leading to complications such as anemia, immunosuppression, gastrointestinal disorders, and organ toxicity. Consequently, there is a growing demand for novel therapeutic systems that can selectively target tumor cells while minimizing adverse effects [2]. Nanotechnology has emerged as a promising solution by enabling the development of efficient drug delivery systems with enhanced therapeutic performance and improved patient safety [3].

Nanoparticle-based drug delivery systems have transformed the field of cancer therapy because of their unique physicochemical properties. Their small size, large surface area, and ability to be functionalized with various biomolecules facilitate targeted drug delivery and controlled release of therapeutic agents [4]. Lipid nanoparticles are particularly attractive owing to their excellent biocompatibility, biodegradability, and ability to encapsulate both hydrophilic and hydrophobic compounds. The incorporation of magnetic nanoparticles into lipid carriers further improves their functionality by allowing external magnetic guidance, enhanced tumor localization, and potential applications in diagnostic imaging [5]. These multifunctional nanoparticles increase drug accumulation at the tumor site while reducing systemic exposure, thereby improving therapeutic efficacy and minimizing treatment-related toxicity [6].

Melanin, a naturally occurring pigment, has recently gained considerable attention as a valuable biomaterial for biomedical applications. It is produced by a wide variety of organisms, including marine bacteria, and possesses remarkable

antioxidant, free radical scavenging, metal-chelating, anti-inflammatory, and photoprotective properties. Unlike synthetic pigments, bacterial melanin can be produced through environmentally friendly fermentation processes with high reproducibility and scalability [7]. Marine bacterial melanin is particularly attractive because marine microorganisms produce structurally unique metabolites that exhibit enhanced biological activities. When conjugated with nanocarriers, melanin improves nanoparticle stability, protects healthy tissues against oxidative damage, and enhances interactions with biological systems [8]. These characteristics make marine bacterial melanin an excellent candidate for the development of advanced nanomedicine platforms for cancer therapy [9].

The combination of marine bacterial melanin with lipid magnetic nanoparticles offers a multifunctional therapeutic strategy capable of improving anticancer efficacy through several complementary mechanisms. Lipid nanoparticles provide a safe and biodegradable carrier, magnetic nanoparticles enable targeted delivery using external magnetic fields, and melanin contributes antioxidant and anti-inflammatory activities that may reduce chemotherapy-associated toxicity [10]. Such integrated nanocomposites have the potential to enhance drug bioavailability, improve tumor-specific accumulation, suppress inflammation, and protect normal tissues while effectively inhibiting tumor growth.

The present study focuses on the development and in vivo evaluation of marine bacterial melanin-conjugated lipid magnetic nanoparticles (M-C-L-M-NPs) as a novel anticancer nanotherapeutic system. Their therapeutic efficacy was assessed using an experimental animal model by evaluating body weight, hematological parameters, inflammatory cytokines, and histopathological changes. The performance of the developed nanoparticles was compared with the standard chemotherapeutic drug 5-fluorouracil (5-FU) to determine their effectiveness. It is anticipated that M-C-L-M-NPs will demonstrate enhanced anticancer activity with improved biocompatibility and reduced systemic toxicity, highlighting their potential as a promising platform for next-generation targeted cancer therapy.

METHODOLOGY

Melanin-Conjugated lipid Magnetic Nanoparticles (M-C-L-M-NPs) were synthesized using the chemical co-precipitation method.

Citrate-capped magnetic iron oxide nanoparticles were synthesized using a modified co-precipitation method. Ferric chloride hexahydrate ($FeCl_3 \cdot 6H_2O$) and ferrous sulfate heptahydrate ($FeSO_4 \cdot 7H_2O$) were dissolved in deionized water at a molar ratio of 2:1 under a nitrogen atmosphere and heated to 60–70°C with continuous stirring to ensure complete dissolution. A 30% ammonium hydroxide solution was then added gradually under vigorous stirring to initiate nanoparticle formation, while sodium hydroxide was used to adjust and maintain the reaction pH at approximately 10. Citric acid was subsequently introduced as a surface-stabilizing agent, enabling its carboxyl functional groups to bind to the Fe_3O_4 nanoparticle surface and minimize particle aggregation through citrate capping. After an additional 30 min of stirring, the magnetic nanoparticles were isolated using an external magnet, repeatedly washed with distilled water to eliminate residual reactants, and dried at 60°C before storage [11]. For the preparation of melanin-loaded lipid nanoparticles, phosphatidylcholine and melanin were dissolved in an organic solvent, whereas an aqueous surfactant solution containing Tween 80 or Poloxamer 188 was prepared separately. The organic phase was slowly introduced into the aqueous phase under high-speed homogenization (10,000–15,000 rpm) to form a stable emulsion. Following solvent evaporation under reduced pressure, melanin-loaded lipid nanoparticles were obtained. Finally, the citrate-capped magnetic nanoparticles were dispersed into the lipid nanoparticle suspension under gentle stirring, allowing their incorporation within the lipid matrix through physical adsorption. The resulting melanin-loaded citrate-capped magnetic lipid nanoparticles (M-C-L-M-NPs) were magnetically separated, washed thoroughly with distilled water to remove unbound components, and stored at 4°C until further characterization and biological evaluation [12].

Characterization of M-C-L-M-NPs

M-C-L-M-NPs were characterised using UV-Vis spectroscopy for surface plasmon resonance analysis, with a BioSpec Nano (Shimadzu). HR-TEM (JEOL) examined surface features and microscopic properties.

In-Vivo Evaluation of Anticancer Activity in a DMBA-Induced Skin Carcinogenesis

Approval for the animal study was obtained from the Institutional Animal Ethics Committee (IAEC; Approval No. JSPC/IAEC/05/12/14-2025), and all experimental procedures were carried out in accordance with the guidelines of the Committee for the Purpose of Control and Supervision of Experiments on Animals (CPCSEA). Male Wistar albino rats were randomly allocated into four groups (n = 6 per group). The normal control group (G-1) received no carcinogenic treatment, while skin carcinogenesis was induced in the disease control group by a single topical application of 100 µg of 12-dimethylbenz[a]anthracene (DMBA) dissolved in 100 µL of acetone onto the shaved dorsal skin, followed by topical application of 1% croton oil (100 µL) three times per week for 16 weeks (G-2). The standard treatment group received the same DMBA/croton oil regimen along with oral administration of 5-fluorouracil at a dose of 20 mg/kg once weekly (G-3). The treatment group was administered DMBA-induced carcinogenesis together with oral M-C-L-M-NPs at a dose of 5 mg/kg body weight, three times per week for the 16-week study period (G-4). Throughout the experiment, body weight, tumor incidence, tumor volume, and tumor latency were monitored at weekly intervals. At the end of the treatment period, the animals were euthanized, and skin tissues were harvested for histopathological examination and biochemical investigations to assess the anticancer potential of the formulated nanoparticles [13].

RESULTS AND DISCUSSION

Melanin-Conjugated lipid Magnetic Nanoparticles (M-C-L-M-NPs) were synthesized using the chemical co-precipitation method

Melanin-conjugated lipid magnetic nanoparticles (M-C-L-M-NPs) were successfully synthesized using a chemical co-precipitation approach followed by lipid encapsulation and melanin incorporation. The synthesis process produced a stable nanoparticle suspension with efficient integration of magnetic iron oxide nanoparticles into the lipid matrix. Citrate capping effectively minimized particle aggregation and improved colloidal stability, while the lipid coating facilitated uniform melanin loading. Magnetic separation confirmed the successful formation of the hybrid nanostructures and enabled efficient purification by removing unbound materials. The prepared nanoparticles exhibited good dispersibility and remained physically stable during storage at 4°C, indicating that the adopted synthesis method was reliable and suitable for producing M-C-L-M-NPs for subsequent physicochemical characterization and biological investigations.

Figure 1: Melanin-Conjugated lipid Magnetic Nanoparticles (M-C-L-M-NPs).

Characterization of M-C-L-M-NPs

UV-UV-Vis spectroscopy analysis of M-C-L-M-NPs

The UV–Visible absorption spectrum of M-C-L-M-NPs demonstrated characteristic absorption bands in the ultraviolet region, confirming the successful formation of the hybrid nanoparticle system. A pronounced absorption peak observed between 250 and 380 nm is attributed to the electronic transitions associated with melanin and the iron oxide core, indicating effective incorporation of both components. The gradual decrease in absorbance toward the visible region suggests good optical stability and minimal light scattering, reflecting a uniform nanoparticle dispersion. These spectral characteristics verify the successful synthesis of M-C-L-M-NPs and support their potential application in biomedical imaging, drug delivery, and anticancer therapy.

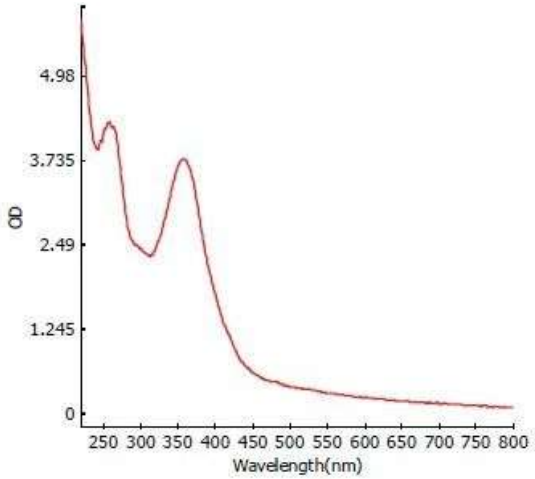

Figure 2: UV–Visible absorption spectrum of melanin-conjugated lipid magnetic nanoparticles (M-C-L-M-NPs). The spectrum exhibits characteristic absorption in the ultraviolet region with a prominent peak between 250–380 nm, confirming the successful incorporation of melanin and magnetic iron oxide nanoparticles into the lipid matrix.

HR-TEM characterization of M-C-L-M-NPs

The HR-TEM characterization confirmed the successful synthesis of melanin-conjugated lipid magnetic nanoparticles (M-C-L-M-NPs) with well-defined nanoscale morphology and structural integrity. The selected area electron diffraction (SAED) pattern displayed distinct concentric diffraction rings, indicating the crystalline nature of the magnetic iron oxide core and suggesting the presence of polycrystalline Fe_3O_4 nanoparticles. HR-TEM micrographs revealed predominantly spherical to nearly spherical nanoparticles with a relatively uniform size distribution and only minor aggregation, demonstrating the effectiveness of citrate capping and lipid encapsulation in improving particle stability. The nanoparticles exhibited clear boundaries with good dispersion within the lipid matrix, indicating successful incorporation of melanin without disrupting the magnetic core structure. The observed particle size was consistent with the nanoscale range expected for biomedical applications, which may facilitate enhanced cellular uptake and drug delivery.

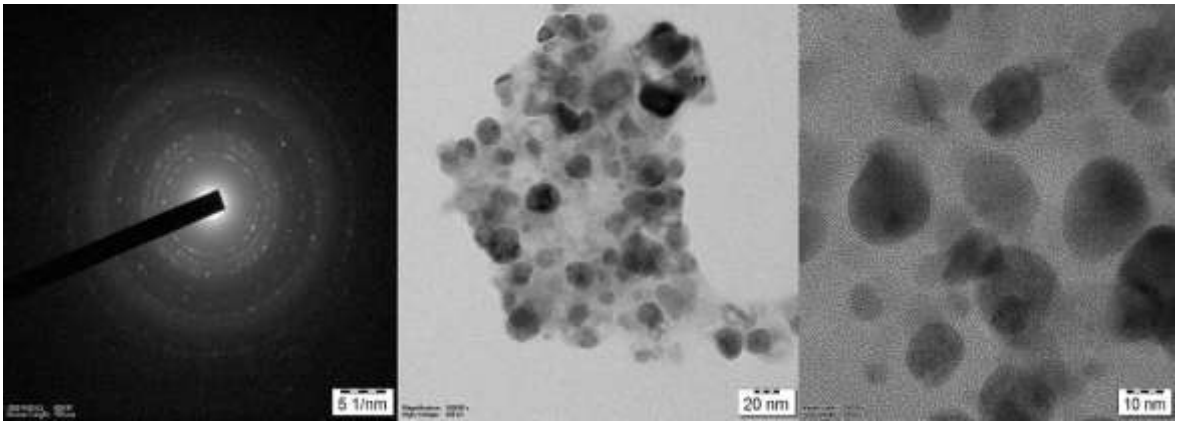

Figure 3: HR-TEM characterization of melanin-conjugated lipid magnetic nanoparticles (M-C-L-M-NPs). (A) Selected area electron diffraction (SAED) pattern showing distinct concentric diffraction rings, confirming the crystalline and polycrystalline nature of the magnetic iron oxide core. (B) HR-TEM micrograph illustrating uniformly distributed nanoparticles with minimal aggregation, indicating effective citrate capping and lipid encapsulation. (C) High-resolution TEM image showing predominantly spherical nanoparticles with well-defined morphology and nanoscale dimensions, demonstrating the successful formation of stable melanin-conjugated lipid magnetic nanoparticles (M-C-L-M-NPs)

.

***In-Vivo* Evaluation of Anticancer Activity of M-C-L-M-NPs in a DMBA-Induced Skin Carcinogenesis**

Body weight of experimental animals

The results presented in the initial body weight analysis demonstrate that all experimental groups had comparable baseline body weights before the commencement of the study, indicating successful randomization and uniform distribution of animals across the treatment groups. The mean body weights of the normal control, cancer control, 5-fluorouracil-treated, and M-C-L-M-NPs-treated groups remained within a narrow range of approximately 147–153 g, with only minimal variation observed among groups. The small error bars further suggest low variability within each group, reflecting consistency in animal selection and handling procedures. Establishing similar initial body weights is essential because it minimizes the possibility that pre-existing differences in nutritional status, growth, or metabolic condition could influence the experimental outcomes. Consequently, any subsequent alterations in body weight, tumor progression, therapeutic efficacy, or biochemical parameters can be more confidently attributed to disease induction or treatment interventions rather than baseline physiological differences. The slightly lower average body weight observed in the cancer control group compared with the other groups is minor and unlikely to be biologically significant, as the overall values remain closely matched. Likewise, the treatment groups exhibited body weights comparable to the normal control, confirming that animals entered the experimental phase under equivalent physiological conditions.

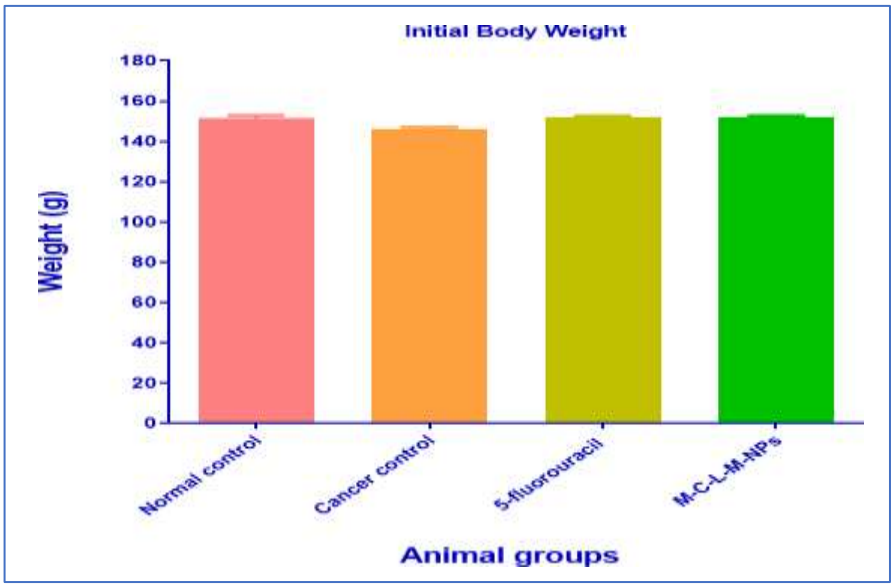

Figure 1: Initial body weight of animals in the normal control, cancer control, 5-fluorouracil (5-FU)-treated, and M-C-L-M-NPs-treated groups before the initiation of the experimental protocol. Data are presented as mean ± SEM (g). No significant differences were observed among the groups at baseline, indicating comparable body weights prior to treatment.

Body weight end of the experiment

The final body weight measurements revealed distinct differences among the experimental groups, reflecting the impact of tumor induction and therapeutic interventions on the overall health status of the animals. The cancer control group

exhibited a marked reduction in body weight compared with the normal control, indicating the adverse effects of cancer progression, including metabolic disturbances, reduced food intake, and increased energy expenditure associated with tumor growth. In contrast, animals treated with 5-fluorouracil demonstrated a substantial improvement in body weight, suggesting that effective suppression of tumor burden contributed to the preservation of nutritional status and general physiological function. Similarly, the M-C-L-M-NPs-treated group-maintained body weights comparable to those of the normal control group and slightly higher than those receiving 5-fluorouracil. This observation indicates that the nanoparticle-based formulation effectively alleviated disease-associated weight loss while supporting normal growth and metabolic balance throughout the experimental period. The maintenance of body weight in treated animals may also reflect reduced systemic toxicity and improved therapeutic efficacy compared with untreated cancer-bearing animals. Since all groups had similar baseline body weights before treatment, the differences observed at the end of the study can reasonably be attributed to the effects of tumor development and the administered treatments.

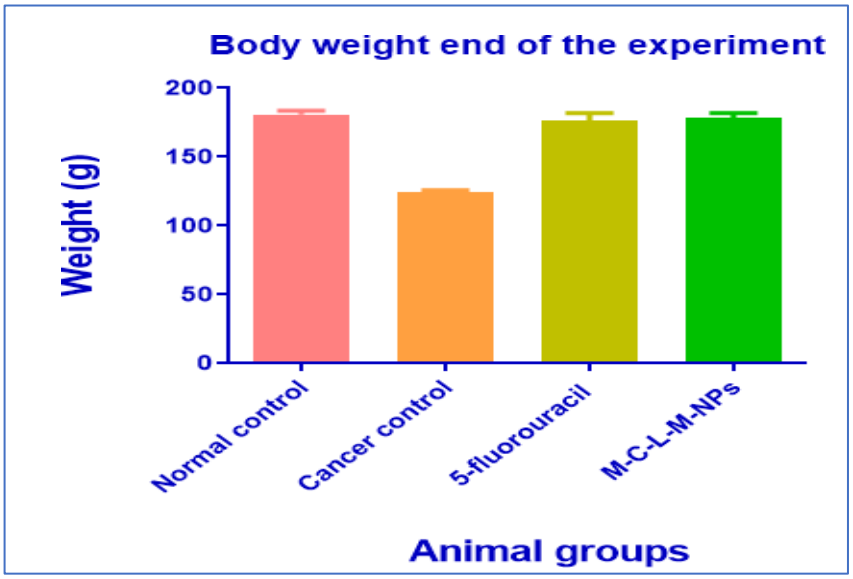

Figure 2: Final body weight of animals in the normal control, cancer control, 5-fluorouracil (5-FU)-treated, and M-C-L-M-NPs-treated groups at the end of the experimental period. Data are presented as mean ± SEM (g). The cancer control group exhibited a marked reduction in body weight, whereas treatment with 5-FU and M-C-L-M-NPs preserved body weight, indicating improved physiological status and therapeutic efficacy compared with untreated cancer-bearing animals.

RBC

The red blood cell (RBC) analysis demonstrated noticeable differences among the experimental groups, reflecting the influence of cancer progression and treatment on hematological status. The normal control group-maintained RBC values within the expected physiological range, indicating normal erythropoiesis and healthy hematological function. Although the cancer control group showed RBC levels comparable to the normal control, a slight decline was observed, suggesting that tumor development may have initiated mild alterations in red blood cell homeostasis. Animals treated with 5-fluorouracil exhibited a further reduction in RBC count, which is consistent with the known myelosuppressive effects of this chemotherapeutic agent. Suppression of bone marrow activity by 5-fluorouracil can impair erythrocyte production, contributing to reduced RBC levels and the potential development of anemia. In contrast, the M-C-L-M-NPs-treated group displayed the highest RBC count among all groups, indicating a protective or restorative effect on hematopoietic function. The improvement in RBC count may be attributed to reduced systemic toxicity, enhanced antioxidant defense, and preservation of bone marrow activity during treatment. Maintaining an adequate RBC count is essential for efficient oxygen transport and tissue metabolism, which supports overall physiological recovery.

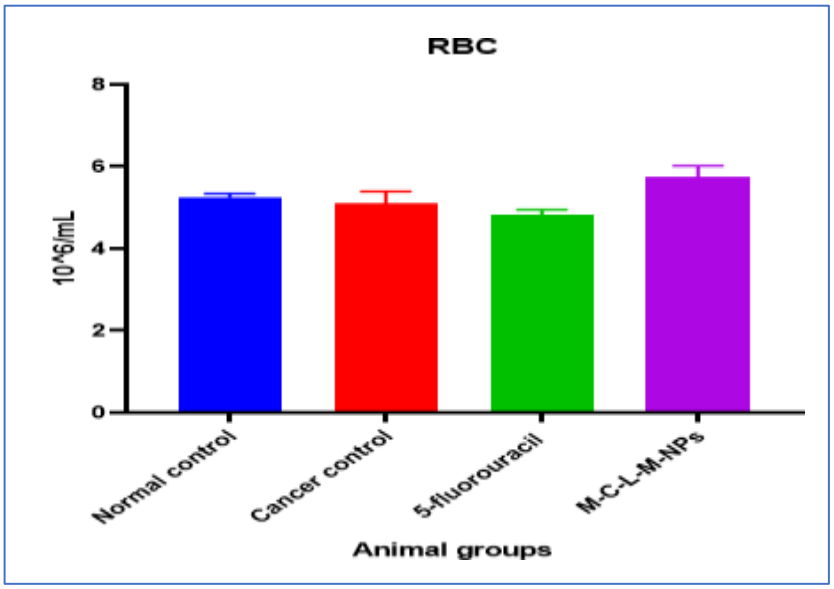

Figure 2: Effect of different treatments on red blood cell (RBC) count in the normal control, cancer control, 5-fluorouracil (5-FU)-treated, and M-C-L-M-NPs-treated groups. Data are presented as mean ± SEM (×10⁶ cells/µL). The M-C-L-M-NPs-treated group exhibited the highest RBC count, whereas the 5-FU-treated group showed a slight reduction, indicating that M-C-L-M-NPs better preserved hematological function during the experimental period.

HB

Hemoglobin (Hb) concentration is an important indicator of the oxygen-carrying capacity of blood and reflects the overall hematological status of experimental animals. In the present study, the cancer control group exhibited a marked reduction in hemoglobin levels compared with the normal control group, indicating the detrimental effects of tumor progression on erythropoiesis and red blood cell function. Cancer-associated inflammation, nutritional deficiencies, and impaired bone marrow activity are well-recognized contributors to reduced hemoglobin concentration in tumor-bearing animals. Treatment with 5-fluorouracil improved hemoglobin levels relative to the cancer control group, suggesting that suppression of tumor growth partially alleviated cancer-induced hematological alterations. However, the hemoglobin concentration remained lower than that observed in the M-C-L-M-NPs-treated group. Animals receiving M-C-L-M-NPs showed the highest hemoglobin levels among all experimental groups, exceedingly even the normal control values. This finding suggests that the nanoparticle formulation effectively preserved erythropoietic function and minimized treatment-related hematological toxicity while enhancing the overall physiological condition of the animals. The improved hemoglobin concentration may also reflect reduced oxidative stress, better nutritional status, and protection of bone marrow cells during treatment. Since adequate hemoglobin levels are essential for efficient oxygen transport and tissue metabolism, the observed improvement indicates enhanced systemic health.

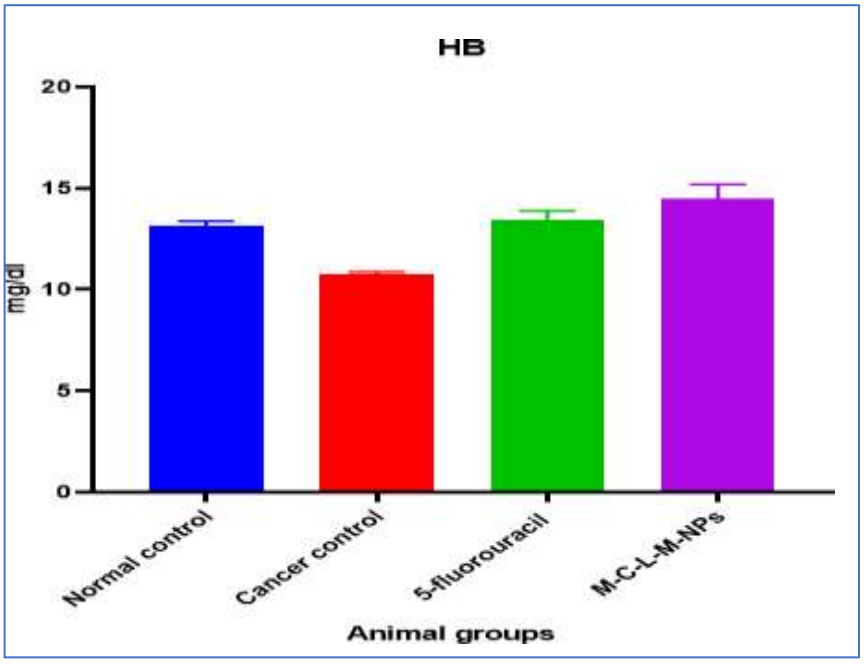

Figure 2: Effect of different treatments on hemoglobin (Hb) concentration in the normal control, cancer control, 5-fluorouracil (5-FU)-treated, and M-C-L-M-NPs-treated groups. Data are presented as mean ± SEM (g/dL). The cancer

control group showed a reduction in hemoglobin levels, whereas treatment with 5-FU and M-C-L-M-NPs improved Hb concentration, with the M-C-L-M-NPs-treated group exhibiting the highest values, indicating enhanced preservation of hematological function.

Inflammatory Marker

Tumor necrosis factor-alpha (TNF-α) is a major pro-inflammatory cytokine that plays a critical role in cancer-associated inflammation, immune regulation, and tissue damage. In the present study, TNF-α levels were highest in the normal control group, whereas the cancer control group exhibited a considerable reduction. Treatment with 5-fluorouracil further decreased TNF-α concentrations, and the M-C-L-M-NPs-treated group demonstrated the lowest levels among all experimental groups. The progressive decline in TNF-α following treatment suggests that both therapeutic interventions effectively modulated inflammatory responses associated with tumor development, with the nanoparticle formulation producing a more pronounced effect. The superior reduction observed in the M-C-L-M-NPs group may be attributed to enhanced drug delivery, sustained therapeutic action, and improved suppression of inflammatory signaling pathways. Nanoparticle-mediated treatment may also reduce oxidative stress and inhibit cytokine production, thereby contributing to a more favorable systemic environment during cancer therapy. Lower TNF-α levels may indicate attenuation of chronic inflammation, which is often linked to tumor progression and tissue injury. The greater anti-inflammatory effect observed with M-C-L-M-NPs compared with conventional 5-fluorouracil suggests improved therapeutic performance while potentially reducing inflammatory complications.

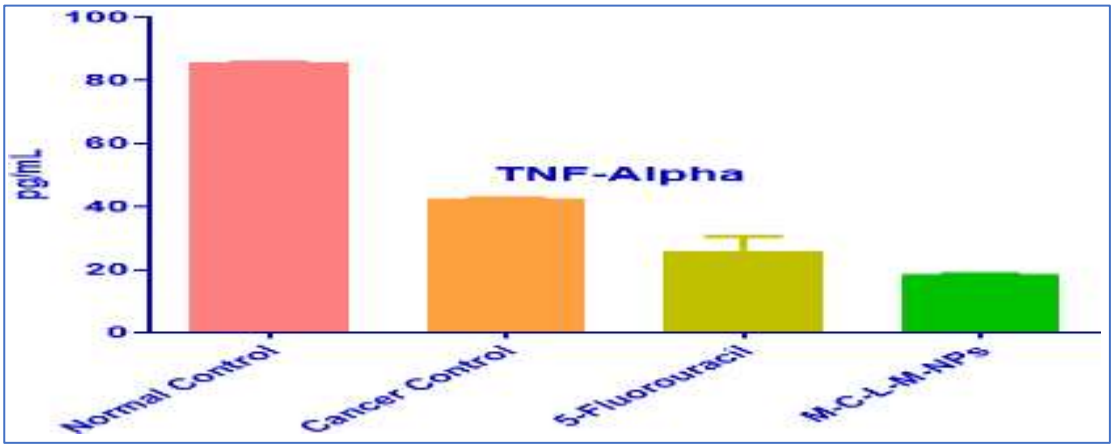

Figure 1: Effect of different treatments on serum tumor necrosis factor-alpha (TNF-α) levels in the normal control, cancer control, 5-fluorouracil (5-FU)-treated, and M-C-L-M-NPs-treated groups. Data are presented as mean ± SEM (pg/mL). Treatment with 5-FU and M-C-L-M-NPs reduced TNF-α levels compared with the cancer control group, with the M-C-L-M-NPs-treated group exhibiting the greatest reduction, indicating enhanced anti-inflammatory activity.

Histopathology

Histopathological examination provided additional evidence of the effects of tumor induction and therapeutic intervention on tissue architecture. The normal control group exhibited well-preserved tissue morphology with intact epidermal and dermal organization, normal cellular distribution, and no evidence of inflammatory cell infiltration or structural abnormalities. In contrast, the cancer control group showed marked histological alterations characterized by disruption of normal tissue architecture, increased cellular density, irregular collagen arrangement, and infiltration of inflammatory cells, indicating extensive pathological changes associated with tumor progression.

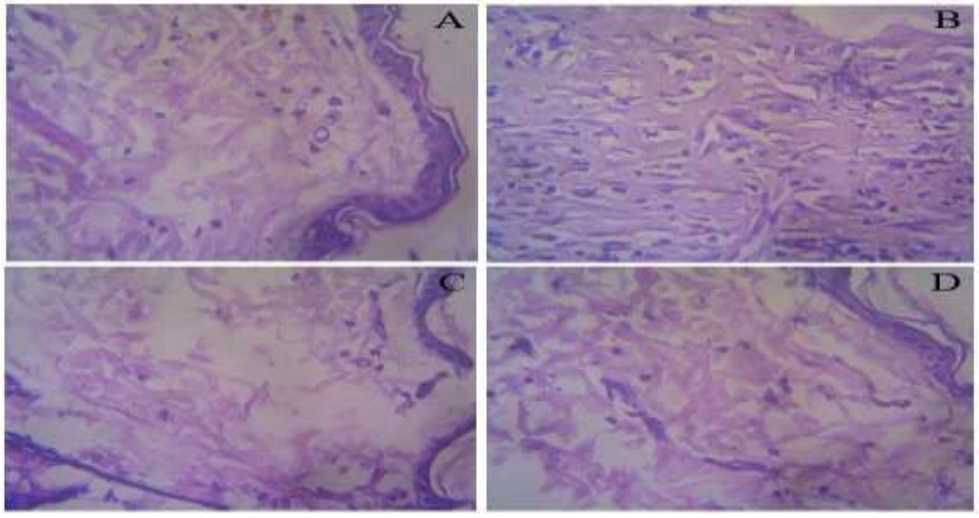

Figure 6. Representative hematoxylin and eosin (H&E)-stained photomicrographs showing histopathological changes in the experimental groups. (A) Normal control showing intact tissue architecture with normal cellular morphology. (B) Cancer control exhibiting disrupted tissue organization, increased cellularity, and inflammatory cell infiltration. (C) 5-Fluorouracil (5-FU)-treated group demonstrating partial restoration of normal histological features with reduced pathological alterations. (D) M-C-L-M-NPs-treated group showing marked preservation of tissue architecture and minimal inflammatory changes, indicating effective protection against cancer-induced tissue damage (H&E staining, original magnification as used in the study).

Treatment with 5-fluorouracil resulted in partial restoration of tissue structure, with reduced cellular abnormalities and diminished inflammatory infiltration compared with the untreated cancer group. Mild degenerative changes and incomplete tissue recovery were still evident. The M-C-L-M-NPs-treated group demonstrated the greatest improvement in histological appearance, with tissue architecture closely resembling that of the normal control. Cellular organization was better preserved, inflammatory infiltration was minimal, and connective tissue integrity appeared substantially restored. These findings suggest that the nanoparticle formulation effectively attenuated tissue damage while promoting structural recovery. The enhanced histological preservation observed in the M-C-L-M-NPs group may be attributed to improved drug delivery, sustained therapeutic activity, and reduced systemic toxicity.

CONCLUSION

The present study successfully demonstrated the synthesis and *in vivo* anticancer potential of marine bacterial melanin-conjugated lipid magnetic nanoparticles (M-C-L-M-NPs) as an innovative nanotherapeutic platform for skin cancer management. The formulated nanoparticles exhibited favorable physicochemical characteristics and significantly improved the overall health status of DMBA-induced skin carcinogenesis animals by preserving body weight, enhancing hematological parameters, reducing inflammatory responses, and restoring normal tissue architecture. Compared with the conventional chemotherapeutic agent 5-fluorouracil, M-C-L-M-NPs showed superior therapeutic performance with improved biocompatibility and reduced treatment-associated toxicity. The combination of marine bacterial melanin, lipid nanoparticles, and magnetic iron oxide created a multifunctional delivery system capable of enhancing therapeutic efficacy while minimizing adverse effects. Histopathological findings further confirmed the protective effect of the nanoparticle formulation against cancer-induced tissue damage. Collectively, these results indicate that M-C-L-M-NPs represent a promising candidate for targeted cancer therapy and provide a strong foundation for future preclinical and clinical investigations aimed at developing safer and more effective nanomedicine-based anticancer treatments.

CONFLICT OF INTEREST: Nil

FUNDING: Nil

ACKNOWLEDGEMENT: The authors thank the Department of Pharmacy, Annamalai University, Annamalai Nagar, Chidambaram–608002, Tamil Nadu, India, for its support.

ABBREVIATIONS

DMBA = 7,12-Dimethylbenz[a]anthracene
M-C-L-M-NPs = Marine Bacterial Melanin-Conjugated Lipid Magnetic Nanoparticles
Fe_3O_4 = Magnetite (Iron Oxide) Nanoparticles
HR-TEM = High-Resolution Transmission Electron Microscopy
SAED = Selected Area Electron Diffraction
UV–Vis = Ultraviolet–Visible Spectroscopy
RBC = Red Blood Cell
Hb = Hemoglobin
TNF-α = Tumor Necrosis Factor-Alpha
5-FU = 5-Fluorouracil
CPCSEA = Committee for the Purpose of Control and Supervision of Experiments on Animals
IAEC = Institutional Animal Ethics Committee
SEM = Standard Error of the Mean
EPR = Enhanced Permeability and Retention
$FeCl_3 \cdot 6H_2O$ = Ferric Chloride Hexahydrate
$FeSO_4 \cdot 7H_2O$ = Ferrous Sulfate Heptahydrate
NH_4OH = Ammonium Hydroxide
NaOH = Sodium Hydroxide

H&E = Hematoxylin and Eosin
rpm = Revolutions Per Minute
µg = Microgram
µL = Microliter
mg = Milligram
kg = Kilogram
g = Gram
°C = Degree Celsius
pg/mL = Picograms per Milliliter
$\times 10^6$ cells/µL = Million Cells per Microliter

REFERENCE

1. Perez, M., Abisaad, J. A., Rojas, K. D., Marchetti, M. A., & Jaimes, N. (2022). Skin cancer: Primary, secondary, and tertiary prevention. Part I. Journal of the American Academy of Dermatology, 87(2), 255–268. https://doi.org/10.1016/j.jaad.2021.12.066
2. Rojas, K. D., Perez, M. E., Marchetti, M. A., Nichols, A. J., Penedo, F. J., & Jaimes, N. (2022). Skin cancer: Primary, secondary, and tertiary prevention. Part II. Journal of the American Academy of Dermatology, 87(2), 271–288. https://doi.org/10.1016/j.jaad.2022.01.053
3. Chandra, J., Hasan, N., Nasir, N., Wahab, S., Thanikachalam, P. V., Sahebkar, A., Ahmad, F. J., & Kesharwani, P. (2023). Nanotechnology-empowered strategies in treatment of skin cancer. Environmental research, 235, 116649. https://doi.org/10.1016/j.envres.2023.116649
4. Borgheti-Cardoso, L. N., Viegas, J. S. R., Silvestrini, A. V. P., Caron, A. L., Praça, F. G., Kravicz, M., & Bentley, M. V. L. B. (2020). Nanotechnology approaches in the current therapy of skin cancer. Advanced drug delivery reviews, 153, 109–136. https://doi.org/10.1016/j.addr.2020.02.005
5. Chaurasiya, M., Kumar, G., Paul, S., Verma, S. S., & Rawal, R. K. (2024). Natural product-loaded lipid-based nanocarriers for skin cancer treatment: An overview. Life sciences, 357, 123043. https://doi.org/10.1016/j.lfs.2024.123043
6. Oswal, K., Tiwary, P., Varghese, R., & Gupta, P. (2026). Solid lipid nanoparticles in skin cancer: A comprehensive review of mechanism, formulation, and therapeutic advances. Pathology, research and practice, 282, 156463. https://doi.org/10.1016/j.prp.2026.156463
7. Riley P. A. (1997). Melanin. The international journal of biochemistry & cell biology, 29(11), 1235–1239. https://doi.org/10.1016/s1357-2725(97)00013-7
8. Solano F. (2020). Photoprotection and Skin Pigmentation: Melanin-Related Molecules and Some Other New Agents Obtained from Natural Sources. Molecules(Basel, Switzerland), 25(7), 1537. https://doi.org/10.3390/molecules25071537
9. Yosri, N., Khalifa, S. A. M., Guo, Z., Xu, B., Zou, X., & El-Seedi, H. R. (2021). Marine organisms: Pioneer natural sources of polysaccharides/proteins for green synthesis of nanoparticles and their potential applications. International journal of biological macromolecules, 193(Pt B), 1767–1798. https://doi.org/10.1016/j.ijbiomac.2021.10.229
10. Poulose, N., Sajayan, A., Ravindran, A., Sreechithra, T. V., Vardhan, V., Selvin, J., & Kiran, G. S. (2020). Photoprotective effect of nanomelanin-seaweed concentrate in formulated cosmetic cream: With improved antioxidant and wound healing properties. Journal of photochemistry and photobiology. B, Biology, 205, 111816. https://doi.org/10.1016/j.jphotobiol.2020.111816
11. Ayyanaar, S., Balachandran, C., Bhaskar, R. C., Kesavan, M. P., Aoki, S., Raja, R. P., Rajesh, J., Webster, T. J., & Rajagopal, G. (2020). ROS-Responsive Chitosan Coated Magnetic Iron Oxide Nanoparticles as Potential Vehicles for Targeted Drug Delivery in Cancer Therapy. International journal of nanomedicine, 15, 3333–3346. https://doi.org/10.2147/IJN.S249240
12. Iannone, M. F., Groppa, M. D., Zawoznik, M. S., Coral, D. F., Fernández van Raap, M. B., & Benavides, M. P. (2021). Magnetite nanoparticles coated with citric acid are not phytotoxic and stimulate soybean and alfalfa growth. Ecotoxicology and environmental safety, 211, 111942. https://doi.org/10.1016/j.ecoenv.2021.111942
13. Lee, P. S., Chiou, Y. S., Chou, P. Y., Nagabhushanam, K., Ho, C. T., & Pan, M. H. (2021). 3'-Hydroxypterostilbene Inhibits 7,12-Dimethylbenz[a]anthracene (DMBA)/12-O-Tetradecanoylphorbol-13-Acetate (TPA)-Induced Mouse Skin Carcinogenesis. Phytomedicine: international journal of phytotherapy and phytopharmacology, 81, 153432. https://doi.org/10.1016/j.phymed.2020.153432.